Accepted Manuscript

The two novel DLL4-targeting antibody-drug conjugates MvM03 and MGD03 show potent anti-tumour activity in breast cancer xenograft models

Shijing Wang, Rihong Zhou, Fumou Sun, Renjie Li, Min Wang, Min Wu

PII: S0304-3835(17)30551-7

DOI: 10.1016/j.canlet.2017.09.004

Reference: CAN 13492

To appear in: *Cancer Letters*

Received Date: 3 July 2017

Revised Date: 28 August 2017

Accepted Date: 10 September 2017

Please cite this article as: S. Wang, R. Zhou, F. Sun, R. Li, M. Wang, M. Wu, The two novel DLL4-targeting antibody-drug conjugates MvM03 and MGD03 show potent anti-tumour activity in breast cancer xenograft models, *Cancer Letters* (2017), doi: 10.1016/j.canlet.2017.09.004.

The two novel DLL4-targeting antibody-drug conjugates MvM03 and MGD03 show potent anti-tumour activity in breast cancer xenograft models

Shijing Wang, Rihong Zhou, Fumou Sun, Renjie Li, Min Wang*, Min Wu**

State Key Laboratory of Natural Medicines, School of Life Science and Technology, China Pharmaceutical University, Nanjing 210009, China

* Corresponding author. Tel.: +86 25 8327 1395; fax: +86 25 8327 1395. E-mail address: minwang@cpu.edu.cn (M. Wang).

** Corresponding author. Tel.: +86 138 5164 6797; fax: +86 25 8327 1395. E-mail address: mickeywu2001@163.com (M. Wu).

Abstract: The anti-human Delta-like 4 (DLL4) monoclonal antibody MMGZ01 has a high affinity to hrDLL4 and arrests the DLL4-mediated human umbilical vein endothelial cell (HUVEC) phenotype, promotes immature vessels, and effectively reduces breast cancer cell growth in vivo. To develop a much more effective therapy, we conjugated MMGZ01 with two small-molecule cytotoxic agents, i.e., monomethyl auristatin E (MMAE) and doxorubicin (DOX), with different linkers to generate antibody–drug conjugates (ADCs), i.e., MMGZ01-vc-MMAE (named MvM03) and MMGZ01-GMBS-DOX (named MGD03), that are more potent therapeutic agents than naked antibody therapeutic agents. The produced anti-DLL4 ADCs can be effectively directed against DLL4 and internalized. Then, the release of MMAE or DOX into the cytosol can induce G2/M or G0/G1 phase growth arrest and cell death through the induction of apoptosis. In vitro, MvM03 was highly potent and selective against DLL4 cell lines. The anti-DLL4 ADCs, particularly MvM03, showed more potent anti-tumour activity than Docetaxel, which is an inhibitor of the depolymerisation of microtubules, in two xenograft breast cancer tumour models. Our findings indicate that anti-DLL4 ADCs have promising potential as an effective therapy for breast cancer.

Keywords: DLL4, Antibody–drug conjugates, Tumour models, MMAE, DOX

1. Introduction

Delta-like 4 (DLL4), which is a key ligand in the Notch signalling pathway, is dramatically confined to the vascular endothelium and is more highly expressed in the tumour vasculature than in normal tissues [1-2]. The over-expression of DLL4 has been identified in many types of cancers, including breast cancer [3], pancreatic carcinoma [4], T-ALL leukaemia [5], glioma [6], bladder cancer [7] and gastric cancer [8]. An anti-DLL4 antibody, i.e., OMP-21M18, has been in a phase I clinical trial that was approved by the FDA in 2010 and has been shown to inhibit tumour growth and decrease cancer stem cell (CSC) frequency in minimally passaged human xenograft models [9].

Antibody-drug conjugates (ADCs) are a class of drugs that use monoclonal antibodies (mAbs) to specifically target tumour-associated antigens as vehicles to deliver covalently attached small-molecule cytotoxic agents into cancer cells [10], and ADCs have been shown to be more potent and promising therapeutic agents than naked antibody therapeutic agents. Several ADCs have entered clinical trials for the treatment of a variety of human cancers [11-12]. Currently, there are two ADCs that are clinically approved by the U.S. Food and Drug Administration (FDA), i.e., Adcetris and Kadcyla,

both of which are stochastically conjugated with small-molecule cytotoxic agents through either cysteine or lysine residues [13-14]. Adcetris, which is an SGN-35, is an anti-CD30 antibody–monomethyl auristatin E (MMAE) conjugate [15]. Kadcyla (T-DM1) consists of the amino acid residue lysine in trastuzumab coupled with the microtubule poison maytansinoid DM1 (a derivative of maytansine) through a non-reducible thioether linkage [16-18]. Treatment with Kadcyla prolonged overall survival by 5–6 months with an objective response rate of 44 %. Although these results are encouraging, they also reveal the limited efficacy of ADCs. On the one hand, certain ADCs, including T-DM1, are highly heterogeneous due to the conjugation sites. On the other hand, the amount of small-molecular toxin that is released into the cytoplasm certainly determines the cell killing potency of the ADC, which may explain the lack of activity of T-DM1 in tumours expressing low levels of HER2 [19]. Therefore, it is likely that an enhancement in ADC-mediated internalization and lysosomal trafficking could significantly improve the cytoplasmic delivery of small molecule toxins, which may result in the killing of cancer cell populations that express a broader range of target proteins, such as CD30 and HER2.

MMAE, which is a synthetic analogue of the natural product dolastatin 10, was synthesized by replacing the amino-terminal valine

of auristatin with a protected form of monomethylvaline [20]. The highly stable peptide linker valine-citrulline (vc), which was selectively cleaved by lysosomal enzymes after internalization [21], was used to produce vc-MMAE. In addition，Doxorubicin (DOX), which is another microtubule inhibitor, was coupled with the linker Gamma-maleimido-butyryloxy Succinimide Ester (GMBS) to synthesize GMBS-DOX.

In the present study, we used a novel anti-human DLL4 monoclonal antibody (MMGZ01), which was previously generated using the hybridoma technique in our laboratory with the expected anti-angiogenesis and anti-tumour effects [22], to develop the ADC drugs MMGZ01-vc-MMAE (named MvM03) and MMGZ01-GMBS-DOX (named MGD03). These drugs were tested and evaluated in a series of in vitro and in vivo experiments, and the novel ADC drugs were found to have anti-tumour activities that were superior to those of the naked antibody. Furthermore, the ADC coupled with MMAE showed higher anti-tumour activity than that coupled with DOX. Thus, these ADCs have a therapeutic potential in treating breast cancer.

2. Materials and methods

2.1 Materials

Human umbilical vein endothelial cells (HUVECs) were obtained from the American Type Culture Collection (ATCC). The human breast adenocarcinoma cell lines (MCF-7 and MDA-MB-231) and HEK-293T cells were preserved in our laboratory. All cell lines were cultured under medium conditions as recommended by the suppliers and incubated in an atmosphere of 5 % CO_2 at 37 °C using standard cell culture techniques. The BALB/c nude mice (female, 6 weeks old) were obtained from Yangzhou University Comparative Medicine Centre, Yangzhou, China. All animals were treated following the standards of Comparative Medicine Centre of Yangzhou University and all animal experiments were carried out in accordance with the Animal of the Ministry of Health of the People's Republic of China (Document No. 55, 2001).

2.2 Preparation of the anti-DLL4 antibody MMGZ01 and ADCs

To determine and obtain the ADC products with the optimal drug / monoclonal antibody ratio (DAR), MMGZ01 was partially reduced with tris (2-carboxyethyl) phosphine hydrochloride (TCEP • HCl, Thermo Scientific, USA) of various concentrations. After incubation, the buffer was exchanged by elution using Sepharose and Sephadex G-25 FF with PBS containing 1 mM diethylenetriamine pentaacetic acid (DTPA, Energy Chemical, Shanghai, China). In total, GMBS

(Thermo scientific, USA) dissolved in dimethyl sulphoxide (DMSO) were added to the DOX • HCl solution (Cayman Chemic, USA) and incubated. The drug linker (vc-MMAE (Chemicals, Shanghai, China) and GMBS-DOX) dissolved in DMSO was then mixed rapidly with the conjugation reaction mixture using a volume calculated to yield a solution containing 10 mol drug linker / 1 mol antibody. The DAR of the ADCs was determined to be approximately 4:1. The mixture was placed on ice for 1 h prior to the exchange buffer by elution using Sepharose and Sephadex G-25 FF equilibrated and concentrated by centrifugal ultrafiltration. The conjugates were then filtered under sterile conditions and stored at -80 °C until use. The characterization of the ADC products was analysed by Western blotting.

2.3 Hydrophobic interaction chromatography (HIC) analysis

The ADCs were analyzed by HIC using an Agilent 1200 HPLC system (Wilmington, DE, USA). The chromatographic separation was performed on a TSK-GEL Butyl-NPR column (4.6 × 35 mm, article size 2.5 μm; TOSOH; Tokyo, Japan) with a mobile-phase gradient elution. For MvM03, the mobile phases were 20 mM phosphate and 1.5 M ammonium sulphate at pH 7.0 in deionized water (solvent A) and 75 % (v/v) 20 mM phosphate and 25 % (v/v) isopropanol at pH 7.0 in deionized water (solvent B). For MGD03, the mobile phases

were solvent A as above and 70 % (v/v) 20 mM phosphate and 30 % (v/v) isopropanol at pH 7.0 in deionized water (solvent B). All solutions were delivered at 0.6 mL/min. The UV detection wavelength was 280 nm and the gradient was started at 10 % of solvent B and then increased to 100 % of solvent B over 20 min. The DAR was determined by a peak area integration.

2.4 Endocytosis and transport of MMGZ01 or ADCs

To assess the internalization of drugs in vitro, flow cytometry and confocal microscopy analyses were performed in HUVECs. HUVECs were divided into eight testing groups and each group was incubated with 200 nM drug. The groups timed at 0, 2, 5, 15, 30, 40, 60 and 90 min were immediately placed on ice, and the internalization was terminated. The flow cytometry assay followed the procedures described above. The internalization percentage (% Internalization) = $[(MFI_{TimeX} - MFI_{background}) / (MFI_{Time0} - MFI_{background})] \times 100$. MFI is an abbreviation of mean fluorescence intensities.

We used a fluorescence microscope to directly observe the internalization effect. Drugs were labelled with the visible fluorescent dye Rhodamine B (Beyotime Institute of Biotechnology, Shanghai, China). HUVECs were cultured overnight and then incubated with 1 μM of RhB-drugs for 2 h. After washing, observations were

performed under a laser confocal microscope (Olympus FV1100). Moreover, the free drugs (50 μM) was mixed with RhB-drugs (1 μM) to evaluate the competitive blocking [23].

2.5 Western blotting assay

The hrDLL4 was separated by SDS-PAGE and electrotransferred onto PVDF membranes (Millipore, Billerica, USA). The treatment method of the membranes and the detection method were described previously in Xu et al. [22]. Finally the protein quantity was detected.

2.6 ADCs affinity assay

The DLL4-binding capacity of the drugs was measured using ELISA. The procedures were described previously in Xu et al. [22]. The absorbance of each well was read at 450 nm and a reference of 630 nm using a plate reader.

2.7 Evaluation of cell killing ability of ADCs in vitro

Cells were seeded at a density of 5000 cells/well in a 96-well plate in triplicate. After incubation, the cells were treated with ADCs (1280, 640, 320, 160, 80, 40, 20, 10, 5, and 1 nm) for 24, 48 and 72 h. Then, the MTT solution was added to each well. MMGZ01, MMAE (Selleckchem, Houston, USA) and Docetaxel were used as controls.

The absorbance of the solution was quantified at 570 and 630 nm using a multiwall plate reader. In addition, the inhibitory rates were expressed as the mean ± standard deviation (SD) of triplicate data points.

2.8 Flow cytometric analysis of ADC binding

In total, 4×10^5 cells were resuspended per sample in PBS containing 2 % FBS. Then, the cells were incubated with drugs, followed by FITC conjugated goat-anti-mouse IgG H+L (Sangon Biotech, Shanghai, China). The cells were analysed in all individual detections. The binding assay was performed using a BD FACS flow cytometry, and the obtained data were processed using FlowJo 7.6 software.

2.9 Induction of apoptosis by ADCs

Cells (3×10^5) were incubated with different treatments. Each cell sample was stained with annexin V-fluorescein isothiocyanate (FITC) and propidium iodide (PI) to differentiate the populations of early apoptotic cells (annexin V^+/PI^-), late apoptotic cells (annexin V^+/PI^+) and necrotic cells (annexin V^-/PI^+) (Sangon Biotech, Shanghai, China). The percentage of apoptotic cells was calculated as the sum of the percentages of the early apoptotic cells and late apoptotic cells.

2.10 Evaluation of ADCs in the cell cycle

The cells were treated as described above. After fixation, each sample was stained with PI solution (Beyotime Biotech, Shanghai, China) and detected using flow cytometry with a FACSCalibur (BD Biosciences, USA). The cell populations at the G0/G1, S and G2/M phases were quantified using the Modfit analysis software.

2.11 Evaluation of the anti-tumour efficacy of ADCs in xenograft tumour models

Tumour cells (1×10^7) were subcutaneously injected as a Matrigel suspension into six-week-old female nude BALB/c mice (Yangzhou University Comparative Medicine Centre, Yangzhou, China) that were used for all xenograft models. The animals were randomly assigned into treatment groups with a mean tumour volume per group of 100–150 mm^3. The tumour size was evaluated once every three days using calliper measurements, and then, the tumour volumes were determined according to the following formula: (length × $width^2$) / 2. Physiological saline was administered as the vehicle control in each model. In the xenograft models of MCF-7 and MDA-MB-231, ADCs (5, 1.5 mg/kg each), MMGZ01 (5 mg/kg), MMAE of corresponding concentration and Docetaxel (10 mg/kg) were intravenously (i.v.)

administered at day 1, 4 and 7, three times totally.

2.12 Immunohistochemistry and immunofluorescence

After administered, the mice were executed at the 21st day. All tumour tissues were fixed and embedded in paraffin. Then, the treatment method of samples was described previously in Xu et al. [22]. For the immunohistochemistry (IHC) straining, the sections were incubated with the primary antibodies anti-Ki67 and anti-cleaved caspase-3 overnight and the corresponding secondary antibody conjugated with HRP. The slides were then incubated with a DAB solution and nuclear counterstained with haematoxylin. The immunofluorescence (IF) staining was performed similarly to the procedure described above. The primary antibodies were anti-CD31 and anti-α-SMA. In addition, the cell chromosome was stained with DAPI. All images were obtained under a Zeiss Axio Vert A1 microscope (Carl Zeiss, Tornwood, NY, USA).

2.13 Statistical analysis

The data are presented as the means ± standard deviation (SD). The statistical analyses were performed using the student’s t-test, and P-values of 0.05 or less were considered statistically significant. The calculation was performed using the GraphPad Prism software

(GraphPad Software Inc., La Jolla, CA, USA).

3. Results

3.1 Characterization of MMGZ01

After purification, the 4-12 % SDS-PAGE analysis showed that MMGZ01 contains a heavy chain band and a light chain band with clear molecular weights of approximately 50 and 25 kDa, respectively (Fig. 1a). The ELISA-based binding assay revealed that this monoclonal antibody had a high affinity to immobilized hrDLL4 (Fig. 1b). A Western blotting assay revealed that MMGZ01 specifically binds to rhDLL4 (Fig. 1c). Moreover, the anti-DLL4 monoclonal antibody MMGZ01 can be efficiently internalized in HUVECs through endocytosis (Fig. 1d, e, f).

3.2 Preparation of the two ADCs

Upon achieving highly efficient production of MMGZ01, we explored the conjugation of MMGZ01 with two linkers and two cytotoxins. MMAE, which inhibits the polymerization of tubulin in dividing cells, was prepared by replacing a protected form of monomethylvaline with the amino-terminal valine during the synthesis of auristatin E [24]. The vc-MMAE contained a p-aminobenzyl carbamate spacer between MMAE and the linker. The

other cytotoxin is DOX, which inhibits the progression of topoisomerase II, an enzyme that relaxes the supercoils in DNA for transcription [25], which reacted with stearic acid-N-hydroxysuccinimide ester (GMBS) to synthesize GMBS-DOX. Both linkers conjugated via a maleimide group with the sulphhydryl group in the mAb. The resultant ADCs were used in these studies and are shown in Fig. 2b, c.

The identities of these ADCs were confirmed by HIC. Since MMGZ01 is an anti-DLL4 IgG2a antibody, each antibody molecule contains five inter-molecule chain disulphide bonds. The reduction of the inter-molecule chain disulphide bonds generates free sulphhydryl groups that permit the conjunction at specific residues using maleimide-containing linkers and produces conjugate compounds at a limited number of defined sites (Fig. 2a). The HIC analysis allowed for the resolution of the conjugates into five major peaks corresponding to zero, two, four, six, and eight drug molecules per antibody (Fig. 3a, b). Furthermore, according to the ultraviolet spectrophotometry (date not shown), we ascertained that the ADCs with the optimal DAR among the ADCs containing the antibody were reduced by different concentrations of TCEP. Consistently with the values of the ultraviolet spectrophotometry (date not shown) and the percentage of the per peak proportion of the HIC, the average DAR of

MvM03 and MGD03 is, respectively, 4.42 and 4.20. The Western blotting assay showed that the ADCs specifically bind to rhDLL4 (Fig. 3c). The ELISA-based binding assay revealed that the novel ADCs had a high affinity to immobilized hrDLL4 even though it was slightly lower than that in MMGZ01 (Fig. 3d). In addition, the ADCs can be efficiently internalized in HUVECs through endocytosis (Fig. 3e, f, g).

3.3 Comparison of binding ability of MMGZ01 and ADCs

Flow cytometry analysis showed compared with the DLL4-negative cell line HEK-293T, ADCs and MMGZ01 showed certain binding signals in DLL4-expressing HUVECs (Fig. 4a). The binding rates of MMGZ01, MvM03 and MGD03 in HUVECs were 31.1 %, 21.8 % and 21 %, respectively, and those in MDA-MB-231 (or MCF-7), which have low level of DLL4 expression, were 9.19 %, 6.30 % and 6.20 % (6.37 %, 3.40 % and 3.25 %), while those in DLL4-negative HEK-293T were 1.64 %, 1.23 % and 2.17 %, respectively, (Fig. 4b).

3.4 Evaluation of cell killing by ADCs in vitro

To compare the potency in vitro, the cells were treated with a series of concentrations of ADCs. In the cell lines, MvM03 exhibited

an enhanced cell killing ability compared to that of MGD03 and a weakened cell killing ability compared to that of Docetaxel (Fig. 5a, b). Thus, the ADCs showed a dose-dependent cell killing effect. Moreover, compared to MDA-MB-231 and MCF-7 cells, the HUVECs treated with ADCs showed a much more potent sensibility and selectivity (Fig. 5c).

3.5 Comparison of cell apoptosis and alterations in cell cycle caused by ADCs in vitro

To further determine whether the observed inhibition effect on proliferation following the treatment with the ADCs was associated with cell apoptosis and alterations in the cell cycle, the cells were treated with appropriate concentrations of ADCs for 24 h and examined by flow cytometry (Fig. 6a, b, c). The ADCs led to an enhanced tumour cell apoptosis in HUVECs. In addition, compared with MGD03, the cell apoptosis rate in MvM03 was higher. However, compared with Docetaxel and MMAE, the cell apoptosis rate in MvM03 was lower. Furthermore, the HUVECs treated with the ADCs showed a stronger susceptibility for the induction of apoptosis than the MDA-MB-231 and MCF-7 cells due to the differences in the DLL4-expression ability of the cells. (Fig. 6d)

The cell cycle analysis indicated that the cells in the G0/G1 phase

were decreased, and those in the G2/M phase were increased after the MvM03 treatment for 24 h compared with those in the negative control group, suggesting that MvM03 can arrest the cells in the G2/M phase. In contrast, the cells treated with MGD03 in the G0/G1 phase were increased, and those in the G2/M phase were decreased, which suggests that MGD03 can arrest cells in the G0/G1 phase. (Fig. 7)

3.6 Comparison of the effect of the ADC treatment on tumour growth, angiogenesis, proliferation, and apoptosis in vivo

To evaluate the efficacy of the anti-DLL4 ADCs in a breast tumour cell line, BALB/c nude mice were xenografted with MDA-MB-231 or MCF-7 tumours. The tumour-bearing mice were treated with the vehicle control, 10 mg/kg Docetaxel, MMAE of corresponding concentration, 5 mg/kg MMGZ01, 5 mg/kg ADCs (high dose group) and 1.5 mg/kg ADCs (low dose group) intravenously. The results showed that the treatment of the tumour-bearing mice with the ADCs (5 mg/kg) induced a significant and durable tumour regression (Fig. 8a). In contrast, the MMGZ01 and Docetaxel treatments only caused a slight delay in tumour growth (Fig. 8a). Compared with the negative control group, the inhibitory rates of MDA-MB-231 tumour growth in animals treated with 5

mg/kg MMGZ01, 10 mg/kg Docetaxel, MMAE of corresponding concentration, 5 mg/kg MvM03, 1.5 mg/kg MvM03, 5 mg/kg MGD03 and 1.5 mg/kg MGD03 were 51.57 %, 42.59 %, 92.90 %, 89.91 %, 70.00 %, 61.90 % and 57.41 %, respectively (Fig. 8b). The same anti-tumour activity was observed in the MCF-7 tumour xenografts. The treatment of mice with 5 mg/kg of MMGZ01 resulted in a 37.31 % decrease in the tumour volume compared with the treatment with normal saline, and the treatment with 10 mg/kg of Docetaxel resulted in a 52.02 % decrease; the treatment with MMAE, 5 mg/kg MvM03 (1.5 mg/kg MvM03) and 5 mg/kg MGD03 (1.5 mg/kg MGD03) resulted in a 94.53 %, 84.92 % (63.97 %) and a 58.73 % (55.10 %) inhibition, respectively (Fig. 8b). Of the two ADCs, MvM03 showed the optimal inhibition of tumour growth. Thus, MvM03 showed a superior anti-tumour effect and safety in vivo in both xenograft tumour models.

The survival rates of the tumour-bearing mice reflect the toxicities of the various tested drugs (Fig. 8c). In the MDA-MB-231 model, after the injection of the high or low dose of MvM03 and MGD03, most mice (five of six) died within 117 or 111 days and 105 or 93 days. In the other mouse groups receiving saline, MMGZ01, MMAE and Docetaxel, however, half of the animals survived for at least 54, 69, 45 and 60 days. Moreover, after the treatment with the high or low

dose of MvM03 and MGD03 in the MCF-7 model, five of six mice died, respectively, within 108, 102, 96 and 87 days. In addition, half of the animals that were treated with saline, MMGZ01, MMAE and Docetaxel survived for approximately 54, 63, 51 and 75 days. 5 mg/kg MvM03 caused a effect to prolong obviously the length of survival. (Fig. 8c)

According to the evolution of the survival rate of mice, the ADCs, particularly MvM03, appeared to have better anti-tumour activity than MMGZ01 and superior security than MMAE in both breast cancer models. Furthermore, the MDA-MB-231 model treated with the ADCs showed a much more potent sensibility and selectivity compared to the MCF-7 model.

The effect of the ADCs on the mitotic index (Ki67) and apoptosis (cleaved caspase-3) in MDA-MB-231 or MCF-7 tumours was detected by IHC staining. An evident reduction in the Ki67 levels and an increase in cleaved caspase-3 were observed after the treatment with the ADCs in both tumours. The treatment with the anti-DLL4 ADCs resulted in a more pronounced reduction in Ki67 in tumour growth compared with that after the MMGZ01 or Docetaxel treatments (Fig. 9a, b). In addition, tumour sections stained for cleaved-caspase 3 to detect apoptosis showed that the ADC treatment caused higher levels of cleaved-caspase 3 than the MMGZ01 or

Docetaxel (Fig. 9c, d). Furthermore, in both MDA-MB-231 (Fig. 9e) and MCF-7 (Fig. 9f) tumour tissues, the MvM03 treatment resulted in a greater decrease in the expression of Ki-67 and a greater increase in cleaved-caspase3 compared with the MGD03 treatment. These results suggest that the ADCs inhibited the tumour cell proliferation and induced apoptosis in the tumour tissues (Fig. 9e, f).

In addition, the percentages of smooth muscle actin (SMA)-positive mural cells after the treatments with the anti-DLL4 ADCs, which were measured using a CD31 antibody and an α-smooth muscle actin antibody, were decreased in both tumour tissues. In particular, the tumours treated with MvM03 were identified with the vehicle control compared with MGD03. As a positive control, the group treated with MMAE showed considerable toxicity. Furthermore, the MDA-MB-231 tumour tissue that was treated with the ADCs showed a significant effect compared with the MCF-7 tumour tissue that was treated similarly, which is consistent with the results of the immunohistochemistry analysis. (Fig. 10a, b, c, d)

Based on a variety of measurements and analyses, it is possible to conclude that the anti-DLL4 ADCs showed significant anti-tumour efficacy and relatively low toxicity in vivo. Therefore, anti-DLL4 ADCs can be selectively localized in the target and deliver high doses of drugs to breast tumour tissues.

4. Discussion

At present, there are several targeting antiangiogenesis monoclonal antibody drugs approved by the FDA including Bevacizumab [26], Ranibizumab [27], Ramucirumab [28] and IMC-18F1 [29]. And DLL4 is an ingredient that is expressed in human arterial endothelial cells, and the blockade of DLL4 in tumours could induce excessive vessels with limited perfusion, consequently preventing tumour growth [30-31]. We have recently shown that an anti-DLL4 mAb, i.e., MMGZ01, meditated the anti-tumour effect through the inhibition of tumour cell proliferation and the promotion of tumour cell apoptosis in MDA-MB-231 and MCF-7 breast cancer xenograft tumours. ADCs provide an efficacious method to deliver a small molecule chemotherapeutic agent to the surfaces of antigen-positive cells through targeted mAb. Once bound to the corresponding antigen, the ADC is internalized, the linker is cleaved and the drug is released into the intracellular microenvironment in which it affects cell killing. By delivering a chemotherapeutic agent to the cell-specific site rather than to antigen-negative normal tissues, the toxicity of the chemotherapeutic agent can be limited, while its therapeutic activity can be focused on the tumour [32]. Hence, antibody affinity and target recognition are

crucial criteria for the development of effective ADC therapies.

In the present study, we focused on making MMGZ01 a more potent anti-tumour agent by coupling MMGZ01 with cytotoxic drugs (MMAE and Doxorubicin) to generate the anti-DLL4 ADCs MvM03 and MGD03. However, the drugs, linkers and coupling technologies are vital for ensuring the optimal efficacy and safety of the ADCs. MvM03 contains a cathepsin B protease-cleavable linker, i.e., valine–citrulline. In addition, MGD03 contains a GMBS linker. MMGZ01, which is an IgG2a antibody, includes five inter-chain disulphides for coupling to toxins [33]. Therefore, MMAE and DOX are coupled to the sulphhydryl groups of the anti-DLL4 mAb via vc or GMBS linkers.

Because the coupling is random, the conjugates are highly heterogeneous, which leads to complicated pharmacokinetics that may be influenced by the drug-load stoichiometry [34]. Notably, conjugates with four drug molecules/mAb have been shown to be more highly active and dramatically less toxic than their counterparts with eight drug molecules/mAb [34]. To minimize the heterogeneity of the ADCs, we explored various reduction–alkylation strategies by adjusting the value of the mAb/TCEP and evaluated the distribution of the types formed. We found that the molecules with two, four, six and eight drugs/mAb accounted for approximately 86 % of the four

types of ADCs investigated, and the proportion of the non-conjugated antibody was less than 10 %. The coupling process was shown to be stable, and the average DAR of MvM03 or MGD03 was 4.42 or 4.20, which revealed that there was no obvious difference in the structural stability of the ADCs in vitro.

In the present work, we newly developed the ADCs MvM03 and MGD03 and performed many experiments. Western blotting was used to test the rhDLL4 specificity of the ADCs. An ELISA was used to detect the affinity of the ADCs. Laser co-focus light microscopy and Flow cytometry were used to reveal the internalization rates of the ADCs to DLL4-positive cells. The results showed extremely similar characterizations of ADCs compared with MMGZ01. Moreover, the ADCs, particularly MvM03, induced cell apoptosis and exhibited a potent cell killing ability in vitro, which may be due to the differences in the linkers and toxicities of the ADCs. In addition, MvM03 successfully blocked cell growth in the G2/M phase of the cell cycle, and MGD03 prevented cell growth in the G0/G1 phase of the cell cycle. Furthermore, MvM03 showed a potent anti-tumour activity in the breast carcinoma xenograft tumour models. Because of the lack of targeting of MMAE, which can invade into most of cells including normal cells, MvM03 at a dose of 5 mg/kg had a much safer characterization compared with MMAE in a survival-time experiment

and induced a significant and durable regression of xenografts, particularly in the MDA-MB-231 model.

To date, several studies have demonstrated that ADCs exhibit promising therapeutic outcomes in mouse models of cancer, and the two ADCs products (Adcetris™ and Kadcyla™) have gained marketing authorization by the FDA for the treatment of certain malignancies in patients. Although these ADCs are very encouraging, a technical deficiency is that the cleavable polypeptide linker is randomly conjugated with the reactive lysine primary amine or cysteine thiol groups of the naked antibodies, which may shrink the therapeutic range in clinical applications due to the lack of control of the toxin concentration. For example, Kadcyla (T-DM1) is highly heterogeneous in terms of the conjugation sites. Trastuzumab contains more than 60 lysine residues in which only a few lysine residues are conjugated with DM1 (DAR is approximately 3.5 in T-DM1), making it challenging to perform ADC characterizations, quality control assessments, and safety/potency assessments [35]. In addition to the slow extravasation of the antibody molecule [36], premature drug release and suboptimal in vivo selectivity [37-39] may result in undesired toxicities and limit their therapeutic efficacy.

Therefore, to overcome these difficulties, site-directed mutagenesis, which is a type of genetic engineering technique that

modifies one or several directed genes allowing small molecule drugs to precisely and quantificationally couple to the directed reactive site of the antibody, may be a solution to yielding more homogeneous ADC products. Currently, the following three methods are used to achieve site-directed conjugation: introducing a reactive cysteine via site-directed mutagenesis, inserting non-natural amino acids as coupling sites via genetic engineering, and coupling via the enzymatic method [40]. Hence, our future work will modify the antibody via site-directed mutagenesis to generate less heterogeneous and more homogeneous ADCs with the optimal efficacy and safety.

In summary, we have developed a unique hrDLL4-targeting ADC, MvM03, which is a highly potent drug for the treatment of DLL4-positive breast cancer malignancies, providing a basis for further development of this anti-DLL4 ADC for the treatment of DLL4-positive cancer diseases.

5. Acknowledgements

This work was supported by funds from the National Natural Science Foundation of China (NSFC81102364, NSFC81273425, NSFC81473125 and NSFC81703404), the Natural Science Foundation of Jiangsu Province (BK20140675), the Fundamental Research Funds for the Central Universities (JKY2011025), the

Project Program of State Key Laboratory of Natural Medicines (China Pharmaceutical University, JKGP201101) and a project funded by the Priority Academic Program Development of Jiangsu Higher Education Institutions.

Conflict of interest: None

6. References

[1] C. Mailhos, U. Modlich, J. Lewis, A. Harris, R. Bicknell, D. Ish-Horowicz, Delta4, an endothelial specific notch ligand expressed at sites of physiological and tumor angiogenesis, Differentiation. 69 (2001) 135–144.

[2] J.R. Shutter, S. Scully, W. Fan, W.G. Richards, J. Kitajewski, G.A. Deblandre, C.R. Kintner, K.L. Stark1, Dll4, a novel Notch ligand expressed in arterial endothelium, Genes Dev. 14 (2000) 1313–1318.

[3] A.M. Jubb, E.J. Soilleux, H. Turley, G. Steers, A. Parker, I. Low, J. Blades, J.L. Li, P. Allen, R. Leek, I. Noguera-Troise, K.C. Gatter, G. Thurston, A.L. Harris, Expression of vascular notch ligand delta-like 4 and inflammatory markers in breast cancer, Am. J. Pathol. 176 (2010) 2019–2028.

[4] M.E. Mullendore, J.B. Koorstra, Y.M. Li, G.J. Offerhaus, X. Fan, C.M. Henderson, S. Bisht, W. Matsui, C.G. Eberhart, A. Maitra, G. Feldmann, Ligand-dependent Notch signaling is involved in tumor initiation and

tumor maintenance in pancreatic cancer, Clin. Cancer Res. 15 (2009) 2291–2301.

[5] S. Indraccolo, S. Minuzzo, M. Masiero, I. Pusceddu, L. Persano, L. Moserle, A. Reboldi, E. Favaro, M. Mecarozzi, G. D. Mario, I. Screpanti, M. Ponzoni, C. Doglioni, A. Amadori1, Cross-talk between tumor and endothelial cells involving the Notch3-Dll4 interaction marks escape from tumor dormancy, Cancer Res. 69 (2009) 1314–1323.

[6] N. El Hindy, K. Keyvani, A. Pagenstecher, P. Dammann, I.E. Sandalcioglu, U. Sure, Y. Zhu, Implications of Dll4-Notch signaling activation in primary glioblastoma multiforme, Neuro Oncol. 15 (2013) 1366–1378.

[7] N.S. Patel, M.S. Dobbie, M. Rochester, G. Steers, R. Poulsom, K.L. Monnier, D.W. Cranston, J.L. Li, A.L. Harris, Up-regulation of endothelial delta-like 4 expression correlates with vessel maturation in bladder cancer, Clin. Cancer Res. 12 (2006) 4836–4844.

[8] S. Ishigami, T. Arigami, Y. Uenosono, H. Okumura, H. Kurahara, Y. Uchikado, H. Okumura, H. Kurahara, Y. Uchikado, T. Setoyama, Y. Kita, Y. Kijima, Y. Nishizono, A. Nakajo, T. Owaki, S. Ueno, S Natsugoe, Clinical implications of DLL4 expression in gastric cancer, J. Exp. Clin. Cancer Res. 32 (2013) 46.

[9] D.C. Smith, P. Eisenberg, R. Stagg, G. Manikhas, A. Pavlovskiy, B. Sikic, A. Kapoun, S.E. Benner, 222 A first-in-human, phase I trial of the

anti-DLL4 antibody (OMP-21M18) targeting cancer stem cells (CSC) in patients with advanced solid tumors, Ejc Suppl. 8 (2010) 73-73.

[10] E.L. Sievers, P.D. Senter, Antibody-drug conjugates in cancer therapy, Annu Rev Med. 64 (2013) 15-29.

[11] W.D. Janthur, N. Cantoni, C. Mamot, Drug conjugates such as Antibody Drug Conjugates (ADCs), immunotoxins and immunoliposomes challenge daily clinical practice, Int. J. Mol Sci. 13 (2012) 16020-16045.

[12] J.M. Lambert, Drug-conjugated antibodies for the treatment of cancer, Brit. J. Clin. Pharmaco. 76 (2013) 248-262.

[13] R.V.J. Chari, M.L. Miller, W.C. Widdison, Antibody–Drug Conjugates: An Emerging Concept in Cancer Therapy, Angew. Chem. Int. Edit. 53 (2014) 3796–3827.

[14] A. Beck, J.M. Reichert, Antibody-drug conjugates: present and future, Mabs. 6 (2014) 15-17.

[15] J. Katz, J.E. Janik, A. Younes, Brentuximab Vedotin (SGN-35), Clin. Cancer Res. 17 (2011) 6428-6436.

[16] P. LoRusso, D. Weiss, E. Guardino, S. Girish, M.X. Sliwkowski, Trastuzumabemtansine: a unique antibody-drug conjugate in development for human epidermal growth factor receptor 2-positive cancer, Clin. Cancer Res.17 (2011) 6437–6447.

[17] S. Verma, D. Miles, L. Gianni, I.E. Krop, M. Welslau, J. Baselga, M.

Pegram, D.Y. Oh, V. Diéras, E. Guardino, L. Fang, M.W. Lu , S. Olsen, K. Blackwell, Trastuzumab emtansine for HER2-positive advanced breast cancer, N. Engl. J. Med. 368 (2013) 1783–1791.

[18] G.D. Lewis Phillips, G. Li, D.L. Dugger, L.M. Crocker, K.L. Parsons, E. Mai, W.A. Blättler, J.M. Lambert, R.V. Chari, R.J. Lutz, W.L. Wong, F.S. Jacobson, H. Koeppen, R.H. Schwall, S.R. Kenkare-Mitra, S.D. Spencer, M.X. Sliwkowski, Targeting HER2-positive breast cancer with trastuzumab-DM1, an antibody-cytotoxic drug conjugate, Cancer Res. 68 (2008) 9280–9290.

[19] J.Y. Li, S.R. Perry, V. Muniz-Medina, X. Wang, L.K. Wetzel, M.C. Rebelatto, M.J.M. Hinrichs, B.Z. Bezabeh, R.L. Fleming, N. Dimasi, H. Feng, D. Toader, A.Q. Yuan, L. Xu, J. Lin, C. Gao, H. Wu, R. Dixit, J.K. Osbourn, S.R. Coats, A Biparatopic HER2-Targeting Antibody-Drug Conjugate Induces Tumor Regression in Primary Models Refractory to or Ineligible for HER2-Targeted Therapy, Cancer Cell. 29 (2016) 117-129.

[20] S.O. Doronina, B.E. Toki, M.Y. Torgov, B.A. Mendelsohn, C.G. Cerveny, D.F. Chace, R.L. DeBlanc, R.P. Gearing, T.D. Bovee, C.B. Siegall, J.A. Francisco, A.F. Wahl, D.L. Meyer, P.D. Senter, Development of potent monoclonal antibody auristatin conjugates for cancer therapy, Nat Biotechnol. 21 (2003) 778–784.

[21] H.D. King, G.M. Dubowchik, H. Mastalerz, D. Willner, S.J. Hofstead, R.A. Firestone, S.J. Lasch, P.A. Trail, Monoclonal antibody

conjugates of doxorubicin prepared with branched peptide linkers: inhibition of aggregation by methoxy triethylene glycol chains, J. Med Chem. 45 (2002) 4336-4343.

[22] Z. Xu, Z. Wang, X. Jia, L. Wang, Z. Chen, S. Wang, M. Wang, J. Zhang, M. Wu, MMGZ01, an anti-DLL4 monoclonal antibody, promotes nonfunctional vessels and inhibits breast tumor growth, Cancer Lett. 372 (2015) 118-127.

[23] L. Ding, C. Tian, S. Feng, G. Fida, C. Zhang, Y. Ma, G. Ai, S. Achilefu, Y. Gu, Small sized EGFR1 and HER2 specifc bifunctional antibody for targeted cancer therapy, Theranostics. 5 (2015) 378-398.

[24] S.O. Doronina, B.E. Toki, M.Y. Torgov, B.A. Mendelsohn, C.G. Cerveny, D.F. Chace, R.L. DeBlanc, R.P. Gearing, T.D. Bovee, C.B. Siegall, J.A. Francisco, A.F. Wahl, D.L. Meyer, P.D. Senter, Development of potent monoclonal antibody auristatin conjugates for cancer therapy, Nat Biotechnol. 21 (2003) 778-784.

[25] Y. Pommier, E. Leo, H. Zhang, C. Marchand, DNA topoisomerases and their poisoning by anticancer and antibacterial drugs, Chem Bio. 17 (2010) 421-433.

[26] N. Ferrara, K.J. Hillan, H.P. Gerber, W. Novotny, Discovery and development of bevacizumab, an anti-VEGF antibody for treating cancer, Nat Rev. 3 (2004) 391-400.

[27] G. Andrew, T. Vivien, A preclinical and clinical review of afibercept

for the management of cancer, Cancer Treat Rev. 5 (2012) 484-493.

[28] J.L. Spratlin, R.B. Cohen, M. Eadens, L. Gore, D.R. Camidge, S. Diab, S. Leong, C. O'Bryant, L.Q.M. Chow, N.J. Serkova, N.J. Meropol, N.L. Lewis, E.G. Chiorean, F. Fox, H. Youssoufian, E.K. Rowinsky, S.G. Eckhardt, Phase I pharmacologic and biologic study of ramucirumab (IMC-1121B), a fully human immunoglobulin G1 monoclonal antibody targeting the vascular endothelial growth factor receptor-2, J. Clin. Oncol. 5 (2010) 780-787.

[29] S.S. Krishnamurthi，P.M. Lorusso，P.H. Goncalves，F. Fox，E.K. Rowinsky, Phase 1 study of weekly anti-vascular endothelial growth factor receptor-1 (VEGFR-1) monoclonal antibody IMC-18F1 in patients with advanced solid malignancies, J. Clin. Oncol. 15 (2008) 431-436.

[30] S. Suchting, C. Freitas, F. le Noble, R. Benedito, C. Breant, A. Duarte, A. Eichmann, The Notch ligand Delta-like 4 negatively regulates endothelial tip cell formation and vessel branching, Proc. Natl. Acad. Sci. U.S.A. 104 (2007) 3225–3230.

[31] I.B. Lobov, E. Cheung, R. Wudali, J. Cao, G. Halasz, Y. Wei, A. Economides, H.C. Lin, N. Papadopoulos, G.D. Yancopoulos, S.J. Wiegand, The Dll4/Notch pathway controls postangiogenic blood vessel remodeling and regression by modulating vasoconstriction and blood flow, Blood. 117 (2011) 6728–6737.

[32] J.A. Francisco, C.G. Cerveny, D.L. Meyer, B.J. Mixan, K. Klussman,

D.F. Chace, S.X. Rejniak, K.A. Gordon, R. DeBlanc, B.E. Toki, C.L. Law, S.O. Doronina, C.B. Siegall, P.D. Senter, A.F. Wahl, cAC10-vcMMAE, an anti-CD30-monomethyl auristatin E conjugate with potent and selective antitumor activity, Blood. 102 (2003) 1458-1465.

[33] T.Y. Yen, H. Yan, B.A. Macher, Characterizing closely spaced, complex disulfide bond patterns in peptides and proteins by liquid chromatography/electrospray ionization tandem mass spectrometry, J. Mass Spectrom. 37 (2002) 15-30.

[34] K.J. Hamblett, P.D. Senter, D.F. Chace, M.M. Sun, J. Lenox, C.G. Cerveny, K.M. Kissler, S.X. Bernhardt, A.K. Kopcha, R.F. Zabinski, D.L. Meyer, J.A. Francisco, Effects of drug loading on antitumor activity of a monoclonal antibody drug conjugate, Clin. Cancer Res.10 (2004) 7063-7070.

[35] X. Yao, J. Jing, X. Wang, C. Huang, D. Li, K. Xie, Q. Xu, H. Li, Z. Li, L. Lou, J. Fang, A novel humanized anti-HER2 antibody conjugated with MMAE exerts potent anti-tumor activity, Breast Cancer Res Tr. 153 (2015) 123-133.

[36] D.R. Mould, K.R.D. Sweeney, The pharmacokinetics and pharmacodynamics of monoclonal antibodies–mechanistic modeling applied to drug development, Curr. Opin. Drug Discov. Devel. 10 (2007) 84–96.

[37] H. Donaghy, Effects of antibody, drug and linker on the preclinical

and clinical toxicities of antibody-drug conjugates, mAbs. 8 (2016) 659-671.

[38] E.R. Boghaert, K.M. Khandke, L. Sridharan, M. Dougher, J.F. DiJoseph, A. Kunz, P.R. Hamann, J. Moran, I. Chaudhary, N.K. Damle, Determination of pharmacokinetic values of calicheamicin-antibody conjugates in mice by plasmon resonance analysis of small (5 microl) blood samples, Cancer Chemoth. Pharm. 61 (2008) 1027–1035.

[39] C. Wei, G. Zhang, T. Clark, F. Barletta, L.N. Tumey, B. Rago, S. Hansel, X. Han, Where did the linker-payload go A quantitative investigation on the destination of the releasedlinker-payload from an antibody-drug conjugate with a maleimide linker in plasma, Anal. Chem. 88 (2016) 4979–4986.

[40] E.S. Zimmerman, T.H. Heibeck, A. Gill, X. Li, C.J. Murray, M.R. Madlansacay, C. Tran, N.T. Uter, G. Yin, P.J. Rivers, A.Y. Yam, W.D. Wang, A.R. Steiner, S.U. Bajad, K. Penta, W. Yang, T.J. Hallam, C.D. Thanos, A.K. Sato, Production of site-specific antibody-drug conjugates using optimized non-natural amino acids in a cell-free expression system, Bioconjugate Chem. 25 (2014) 351-361.

Fig. 1 Characterization of MMGZ01. **a** Gradient SDS-PAGE (4–12 %) analysis of MMGZ01. 1 Molecular weight markers (top to bottom: 200, 150, 120, 100, 85, 70, 60, 50, 40, 30, 25, 20, 15 and 10 kDa); 2

MMGZ01 (non-reduced); 3 MMGZ01 (reduced). **b** hrDLL4-binding test for the affinity of MMGZ01 (EC_{50} value of MMGZ01 was 32 nM). **c** Western blot assay of rhDLL4 detected by MMGZ01. **d** Laser confocal fluorescence microscopy images of HUVEC cells incubated with the RhB-MMGZ01 fluorescent probe, with or without a blocking dose of free MMGZ01. **e** Mean fluorescence intensity of HUVEC cells treated with RhB-MMGZ01 probes, compared to blocking with free MMGZ01. **f** MMGZ01 internalized into HUVEC cell rapidly within about 40 min. The internalization rate was stabilizing at 60-90 min. Data were given as the mean ± SD (n = 3). ***$p < 0.001$. NS: no significance.

Fig. 2 Structures of antibody–drug conjugates. Conjugates were prepared by controlled partial reduction of internal anti-DLL4 antibody MMGZ01 disulfides with TCEP, followed by addition of the maleimide-vc-linker-MMAE or the maleimide-GMBS-DOX. Stable thioether-linked ADCs were formed by the reaction of the maleimides present on the drugs with the free sulfhydryl groups on the monoclonal antibodies (mAbs), with expected drug loads arising in intervals of 2, 4, 6, 8 and 10 with related possible positional isomers. **a** Illustration of ADCs with different drug load distributions. **b** The equation to compound GMBS-DOX. **c** Molecular structures of ADCs.

Fig. 3 Characterization of antibody–drug conjugates. **a** and **b** Hydrophobic interaction chromatography (HIC) analysis of ADCs on a butyl-NPR column yielded five predominant peaks corresponding to mAbs containing zero, two, four, six, and eight drug molecules. **c** Western blot assay of the rhDLL4 specifically detected by anti-DLL4 ADCs. **d** hrDLL4-binding test for the affinity of anti-DLL4 ADCs (EC_{50} value of MvM03 was 42.3 nM and EC_{50} value of MGD03 was 40.1 nM). **e** Anti-DLL4 ADCs internalized into HUVEC cell rapidly within 40 min. The internalization rates were stabilizing at 90 min. **f** Laser confocal fluorescence microscopy images of HUVEC cells incubated with the RhB-MvM03 or RhB-MGD03 fluorescent probe, with or without a blocking dose of free MvM03 or MGD03. **g** Mean fluorescence intensity of HUVEC cells treated with RhB-ADCs probes, compared to blocking with free ADCs. Data were given as the mean ± SD (n = 3). ***$p < 0.001$. NS: no significance.

Fig. 4 The binding capacity of ADCs. **a** Flow cytometry analysis of binding of rhDLL4-expressing cells HUVEC or low-expressing cells (MDA-MB-231 and MCF-7) with anti-DLL4 ADCs and naked antibody MMGZ01. HUVEC, MDA-MB-231, MCF-7 and HEK-293T cells (a hrDLL4 negative cell line) were analyzed using a flow cytometer. **b** Quantifcations of the binding rate of ADCs. The cells were incubated

with anti-DLL4 ADCs or MMGZ01. MvM03 and MGD03 exhibited similar binding rates to HUVEC cells (21.8% and 21.0% respectively), and low bindings to MDA-MB-231 (6.30% and 6.20% respectively) and MCF-7 (3.40% and 3.35% respectively) were observed. As a control, HEK-293T groups showed lower binding rates of MvM03 (1.23 %) and MGD03 (2.17 %).Data were presented as the mean ± SD, n = 3, **p < 0.001, ***p < 0.0001. NS: no significance.

Fig. 5 In vitro cytotoxicity and selectivity of anti-DLL4 ADCs. The cytotoxicity of ADCs was assessed by MTT assay after 72 h of continuous exposure to MMGZ01, anti-DLL4 ADCs, or control Docetaxel. **a** The percentage of cell inhibition relative to untreated control HUVEC, MDA-MB-231 and MCF-7 cells was calculated for each ADC concentration. Anti-DLL4 ADCs induced potent anti-proliferative effects in HUVEC cells and significantly inhibit the growth of cells in comparison to MMGZ01. **b** In vitro potency of anti-DLL4 ADCs compared to the naked antibody (MMGZ01) after 72 h exposure (IC_{50} values). Data are presented as mean ± SD.

Fig. 6 ADCs induces apoptosis of HUVEC, MDA-MB-231 or MCF-7 cells. HUVEC (**a**), MDA-MB-231 (**b**) and MCF-7 (**c**) cells were separately treated with corresponding concentrations of Docetaxel,

MMAE, MMGZ01and ADCs for 24 h analyzed by flow cytometry following staining with Annexin V-FITC and PI. Among them, the percentage of cells in each quadrant was indicated. **d** Quantitative analysis of apoptosis assay. Data were presented as the mean ± SD, n = 3, *p< 0.05, **p< 0.001, ***p< 0.005. NS: no significance.

Fig. 7 MvM03 induces the G2/M phase arrest and MGD03 induces the G0/1 phase arrest in HUVEC, MDA-MB-231 and MCF-7 cells. Cell cycle analyzes HUVEC (**a**), MDA-MB-231 (**b**) and MCF-7 (**c**) cells which were incubated with certain concentrations of MMAE, Docetaxel, MMGZ01 and ADCs for 24 h and stained with PI. The percentage of cells in each phase was indicated. **d** Quantitative analysis of cell cycle assay. Data were presented as the mean ± SD, n = 3, **p < 0.005, ***p < 0.0001. NS: no significance.

Fig. 8 Comparison of efficacy of anti-DLL4 ADCs in MDA-MB-231 and MCF-7 xenograft models. BALB/c mice were injected s.c. with MDA-MB-231 or MCF-7 cells. **a** and **b** Tumor inhibition rates of different dosage groups. 5 mg/kg MvM03 resulted in significant tumor growth inhibition. **c** Survival rates of tumor-bearing mice in different groups. 5 mg/kg MvM03 caused a effect to prolong obviously the length of survival. The arrows indicate dosing days. Data are presented as the

mean ± SD, n = 6, **p < 0.01, ***p < 0.0001. NS: no significance.

Fig. 9 Anti-DLL4 ADCs inhibits cell proliferation and induces apoptosis in MDA-MB-231 and MCF-7 tumors. **a** and **b** IHC staining of Ki-67 (anti-Ki67 antibody) for proliferation in paraffin sections of xenografted tumor. Scale bar= 50 μm. **c** and **d** IHC staining of cleaved-caspase 3 (anti-cleaved caspase 3) for apoptosis in paraffin sections of xenografted tumor. Scale bar= 50 μm. **e** and **f** Quantifcations of Ki67 or cleaved caspase-3 positive cells per field. Data are given as the mean± SD (n= 3). Data are given as the mean ± SD (n= 3). *p< 0.05, **p< 0.001, ***p< 0.0001. NS: no significance.

Fig. 10 Anti-DLL4 ADCs block angiogenesis and indirectly inhibit tumor growth in MDA-MB-231 and MCF-7 tumors. **a** and **b** Tumor vessel number and perfusion were determined by an antibody to SMA (green) for mural cells and a CD31 antibody (red) for vessel staining. Scale bar= 50 μm. **c** and **d** Quantifcations of mature (CD31+/α-SMA+) or immature (CD31+/α-SMA−) vessels per field. Data are given as the mean± SD (n= 3). *p< 0.05, **p< 0.001, ***p< 0.0001. NS: no significance.

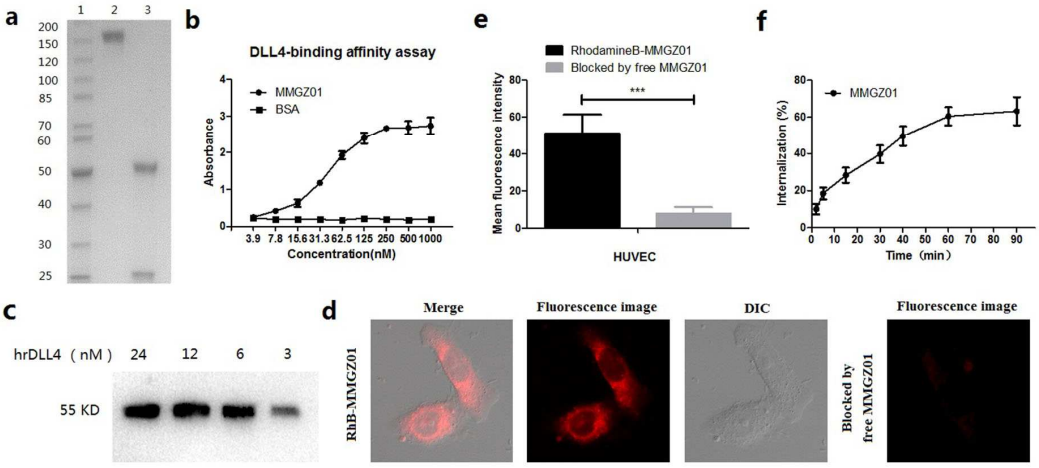

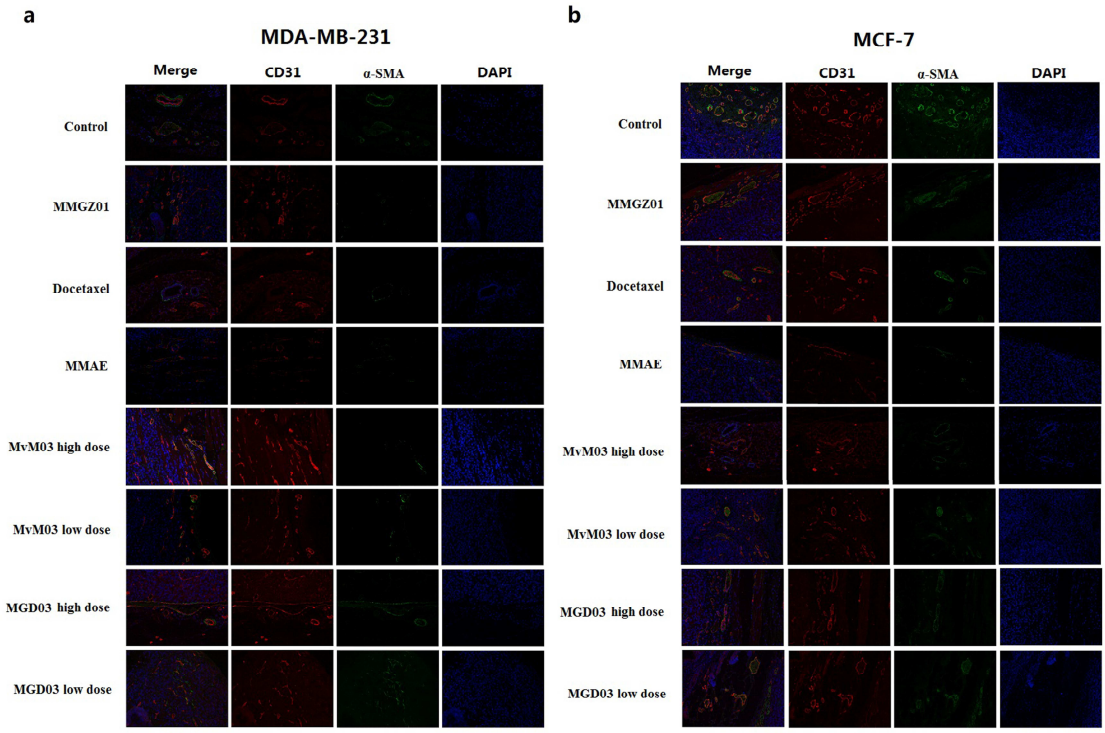

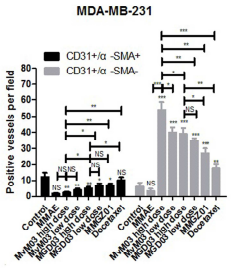

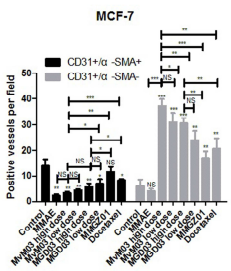

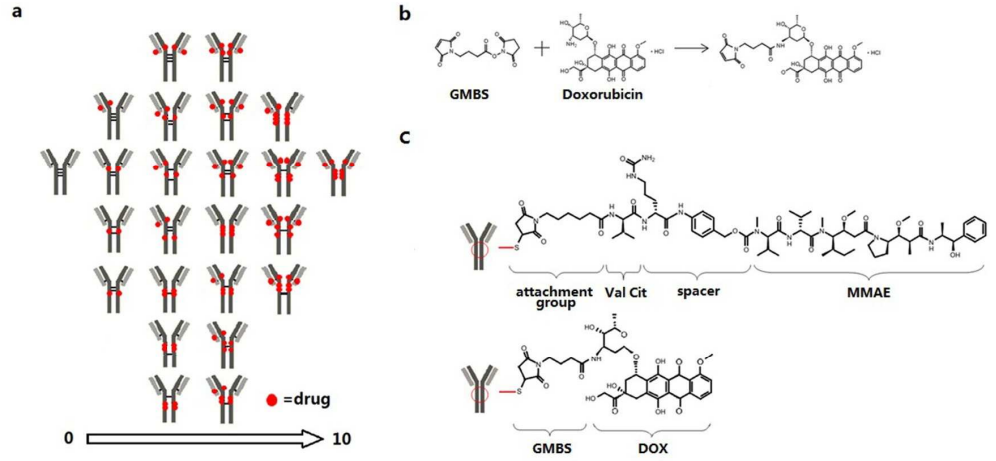

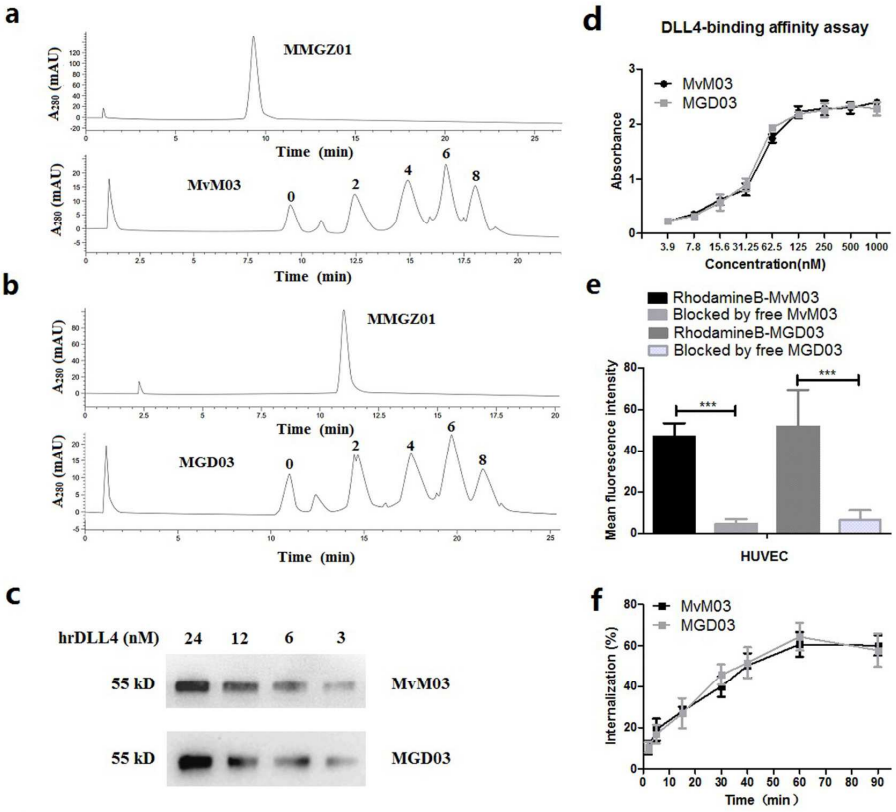
a
MMGZ01
MvM03
Time (min)
b
MMGZ01
MGD03
Time (min)
c
hrDLL4 (nM) 24 12 6 3
55 kD
MvM03
55 kD
MGD03
d
DLL4-binding affinity assay
MvM03
MGD03
Absorbance
Concentration(nM)
e
RhodamineB-MvM03
Blocked by free MvM03
RhodamineB-MGD03
Blocked by free MGD03
Mean fluorescence intensity
HUVEC
f
MvM03
MGD03
Internalization (%)
Time (min)
g
Merge
Fluorescence image
DIC
Fluorescence image
RhB-MvM03
Blocked by free MvM03
RhB-MGD03
Blocked by free MGD03

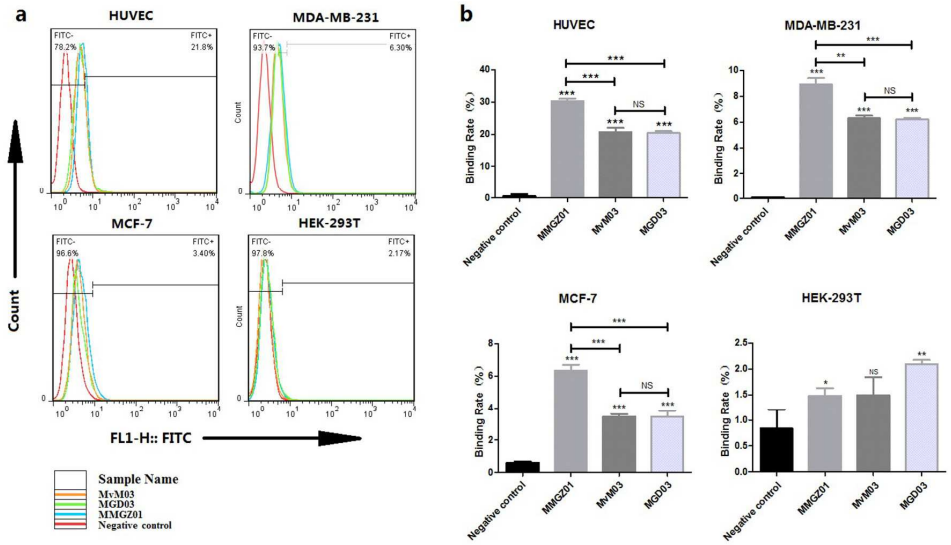

a

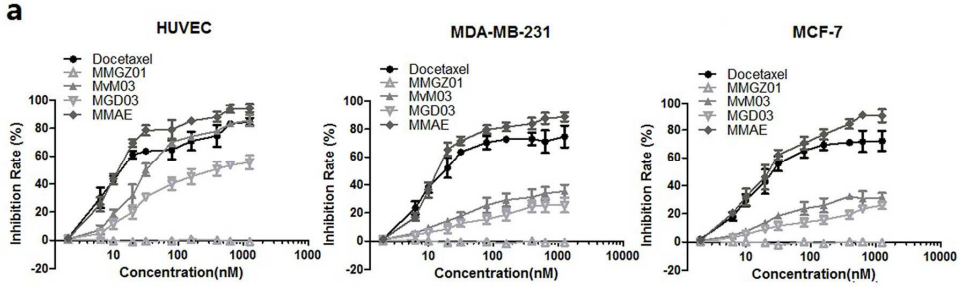

b

IC_{50} (nM)	MvM03	MGD03	Docetaxel	MMAE
HUVEC	39.757 ± 0.700	43.121 ± 1.610	9.622 ± 1.927	10.16 ± 0.199
MDA-MB-231	> 1000	> 1000	10.04 ± 0.776	10.67 ± 0.445
MCF-7	> 1000	> 1000	22.12 ± 1.000	13.37 ± 1.455

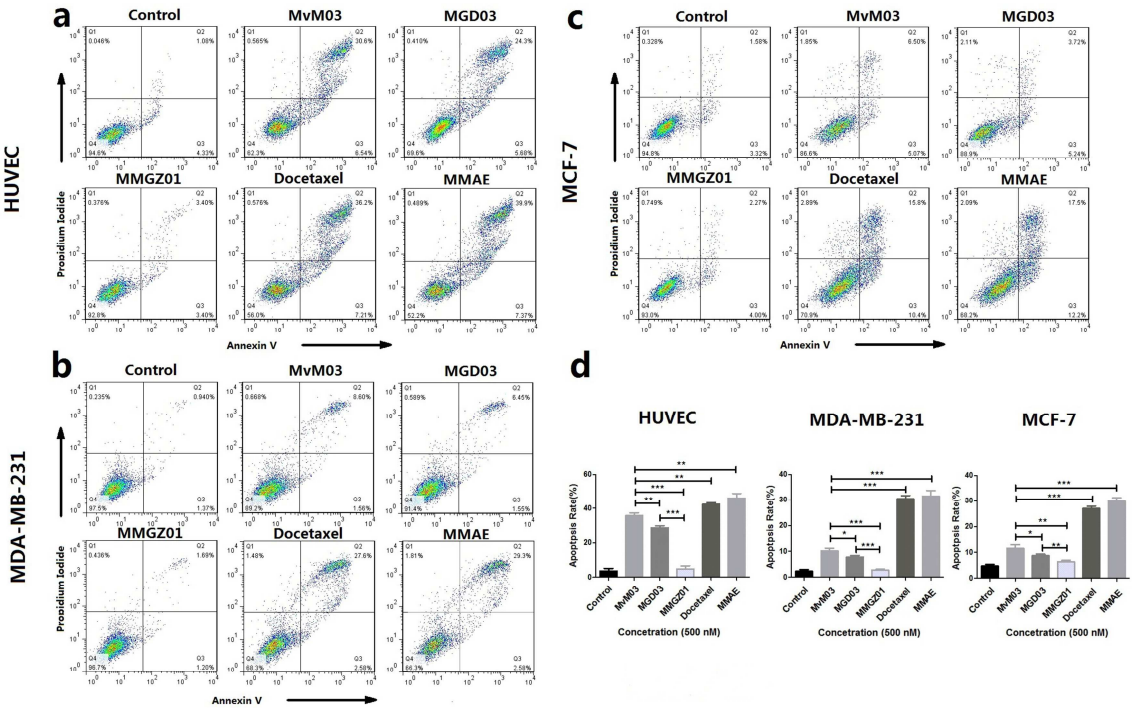

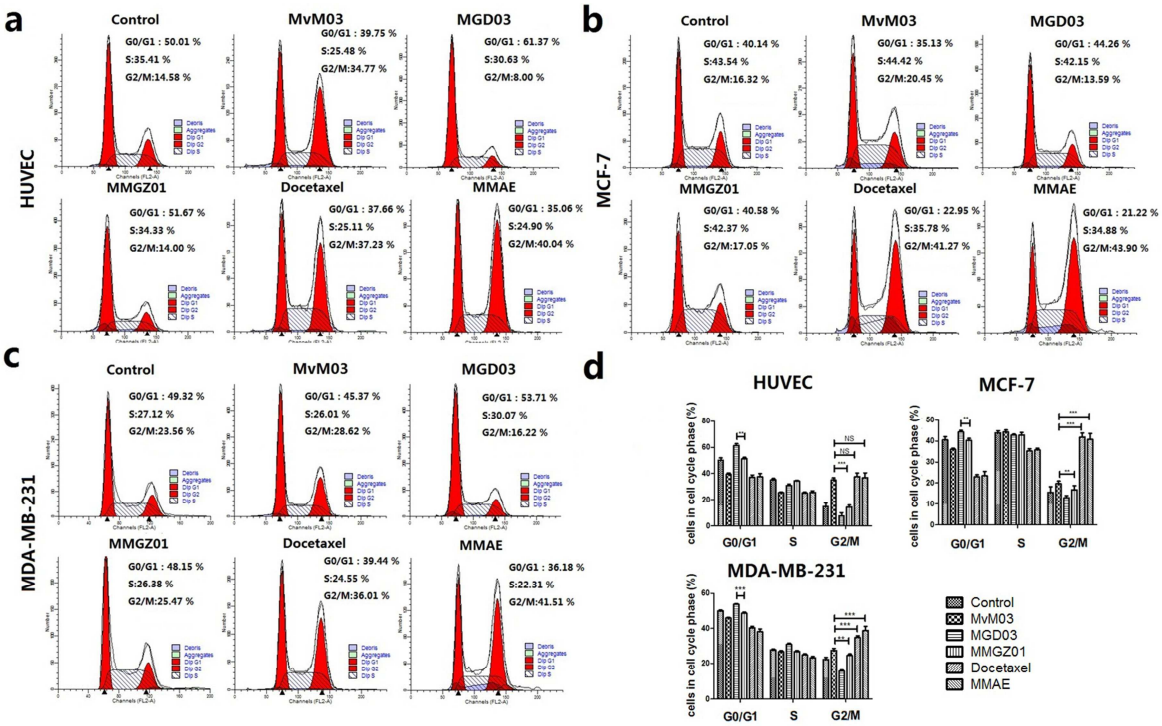

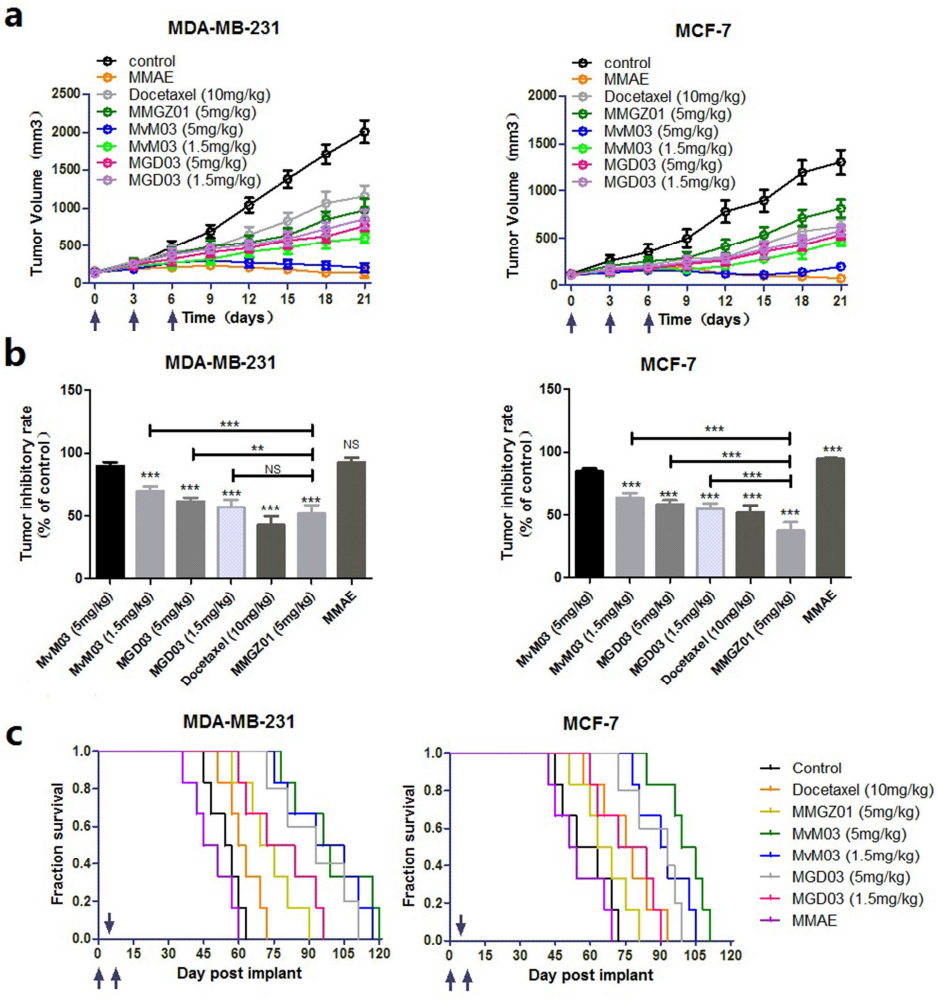
a
MDA-MB-231
MCF-7
control
MMAE
Docetaxel (10mg/kg)
MMGZ01 (5mg/kg)
MvM03 (5mg/kg)
MvM03 (1.5mg/kg)
MGD03 (5mg/kg)
MGD03 (1.5mg/kg)
Tumor Volume (mm3)
Time (days)
b
MDA-MB-231
MCF-7
Tumor inhibitory rate (% of control)
NS
MvM03 (5mg/kg)
MvM03 (1.5mg/kg)
MGD03 (5mg/kg)
MGD03 (1.5mg/kg)
Docetaxel (10mg/kg)
MMGZ01 (5mg/kg)
MMAE
c
MDA-MB-231
MCF-7
Fraction survival
Day post implant
Control
Docetaxel (10mg/kg)
MMGZ01 (5mg/kg)
MvM03 (5mg/kg)
MvM03 (1.5mg/kg)
MGD03 (5mg/kg)
MGD03 (1.5mg/kg)
MMAE

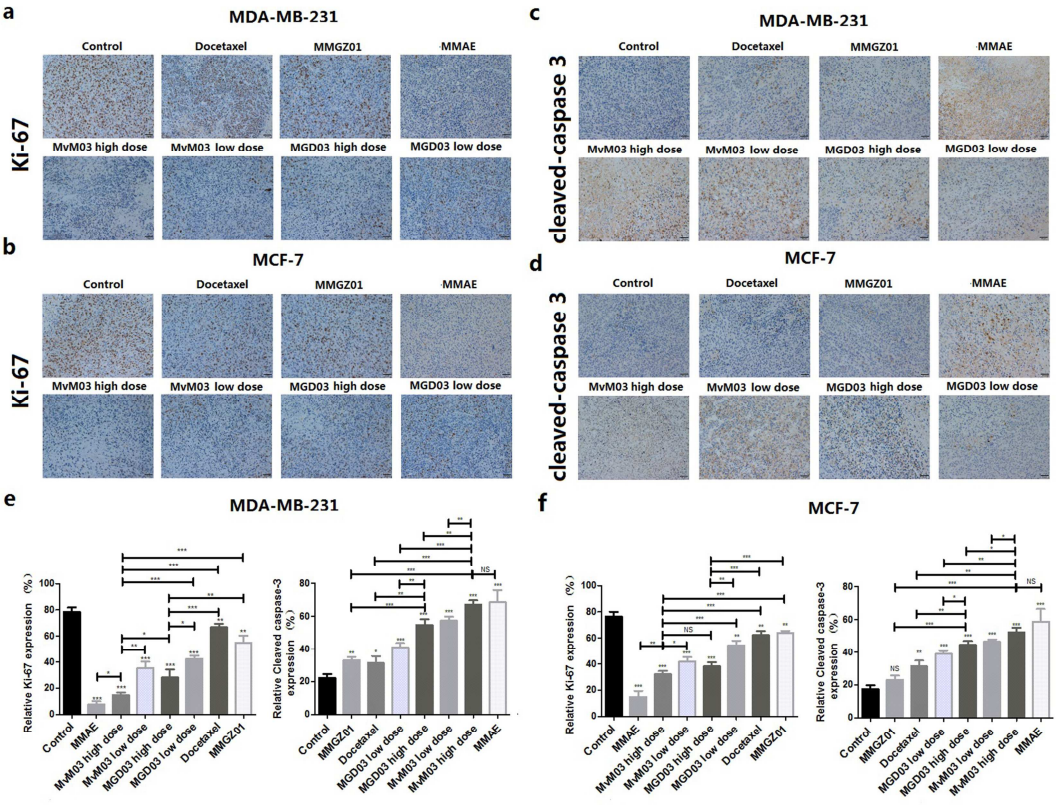

Highlights

1. A novel anti-DLL4 monoclonal antibody MMGZ01 couples with two drugs, i.e. MMAE and DOX to develop two novel ADCs.
2. The two anti-DLL4 ADCs help improve targeting activity and reduce toxicity of MMAE and DOX.
3. The anti-DLL4 ADCs have superior anti-tumour activities in vivo.